Izzeldin Idris Abdalla[1], Ezrann Z. Zainal A.[2], Anwarudin A.R.T[3], Firmansyah[4], A. Rashid A. Aziz[5,*] M.R. Heikal[6]

J. Electrical Systems 13-3 (2017): 489-502

Regular paper

Cogging Force Issues of Permanent Magnet Linear Generator for Electric Vehicle

Alternatives to hydraulic drives that used on vehicles are necessary in order to reduce the Carbon dioxide (CO_2) emission and oil consumption. Hence better performance and efficiency of the vehicles can be achieved by using free piston engine, in which the piston reciprocate linearly with a permanent magnet linear generator (PMLG) without the need of a crankshaft. The PMLG has high performance, but suffering from the cogging force. The cogging force induces undesired vibration and acoustic noise and makes a ripple in the thrust force. Moreover, the cogging force deteriorates the control characteristics, particularly in terms of the position control and speed precisely. This paper proposes Somaloy to replace the laminated silicon steel sheets in order to reduce the cogging force in a PMLG. Through a finite-element analysis, it has been shown that, the stator core made of Somaloy minimizes the cogging force of the PMLG, moreover, giving larger flux-linkage and back-electromotive force (B-EMF), respectively.

Keywords: Cogging force, ferromagnetic materials, Finite element analysis, permanent magnet linear generator.

Article history: Received Received 19 March 2016, Accepted 18 June 2017

1. Introduction

Significant amounts of Carbon dioxide (CO_2) emission and other pollutants are produced by the extensive use of fossil fuels as an energy source for both land and sea-based transport [1]. Within the automotive industry, there are many kinds of research have been done to reduce the oil consumption which causes environmental problems and high cost. The hybrid electric vehicle is one of currently studied solutions [2, 3].

The configuration of the conventional internal combustion engines powering the hybrid electric vehicles generally used the crank mechanism, which restricts the motion of the piston. Moreover, the major part of the total friction losses occurring in the conventional combustion engine because of the crank mechanism [4, 5]. Besides, the crank mechanism limits the range of the compression ratio of the engine. Hence better performance and efficiency of the conventional engine can be achieved by eliminating the crank mechanism. This can easily be realized by using free piston engine, in which the piston reciprocate linearly with PMLG without the need of a crankshaft [6-8].

The free-piston engine converter composed of a permanent magnet linear generator coupled to a free-piston engine. Recently, this technology is being a major of concern of a number of researchers worldwide. The flexibility and easy controllability as well as the

* Corresponding author: A. Rashid A. Aziz, Centre for Automotive Research and Electric Mobility,
E-mail: rashid@utp.edu.my
[5]Universiti Teknologi PETRONAS
32610 Bandar Seri Iskandar, Perak, Malaysia

high efficiency of electrical machines, make them an interesting concept [9, 10]. The growing interest of the automotive industry in the technology of electric hybrid vehicles is a driving force behind the interest in free-piston engine generators. The single piston and dual piston of free-piston engine generator designs have been reported. The use of the electric machine as a rebound device has been proposed in order to replace a bounce chamber in the single piston engine. The use of the electric machine in a motoring mode to aid engine control and for starting is possible by implementing an appropriate power electronics control [8, 11].

Mainly, there are four different approaches to producing a linear energy conversion. The first approach is to use the electrostatic properties. Thus, a maximum force density of about 16 N/m^2 can be obtained. The second approach of which is of the interest for this study, is to produce a linear energy conversion by an electromagnetic way. The third and fourth approaches based on mechanical friction use the piezoelectric or magnetostrictive properties to interact with the translator [12].

The developments based on the PMLG are very likable owing to efficient electromagnetic performance, despite, suffers from the cogging force. This force produces due to the attraction between ferromagnetic core and magnetic with zero current in the winding of the machine [13, 14]. The periodic waveform of the cogging force is depending on the relative position of the translator. When the excitation current assigned to the winding of the machine, the cogging force will be added to a thrust force. The cogging force makes a ripple in thrust force. The ripple resulted by the cogging force will deteriorates the position control and precise speed in many applications. The low-speed applications are more suffering from such ripple; moreover, it produces undesirable acoustic noises and vibrations. Thus, at the design stage must be minimized [13]. Numbers of techniques have been used to reduce the cogging force in permanent magnet machines, but most of these techniques contribute to the reducing of the actual electromagnetic performance. Alternatively, air-cored PMLGs are preferred in terms of unavailability of cogging force, lightweight and simplicity but they have limitations in electromagnetic performance [15-17]. Table 1 gives the comparisons of the slotted and slotless linear electrical machines [18].

Table 1: Slotted versus slotless linear electrical machines

Quantity	Slotted	Slotless
Higher efficiency at lower speed range	√	
Higher thrust density	√	
Lower input current	√	
Higher efficiency at higher speed range		√
Lower cogging force		√
Minimum cost of the winding		√
Less use of PM material	√	
Minimum noise		√

An accurate and fast calculation of the magnetic field distributions created by the PMs are necessary for many electromagnetic machines, they can provide more efficient design and execution of such machines, subsequently, higher performance can be obtained [19]. However, numerous modeling methods are exist for prediction and analysis the

electromagnetic behaviour of the electric machines. These methods vary from simple and accurate to a complicated and time-consuming models [20]. The finite element analysis (FEA) is offering many features, thus, it is widely used for the modeling and simulation of the electrical machines. However, the FEM empowers us to perform a complicated analysis of electrical machines in a minimum estimation time.

This paper presents the electromagnetic analysis and cogging force investigation of a PMLG using two different ferromagnetic materials for the stator core by using finite element analysis (FEA) software ANSOFT Maxwell.

2. Problem formulation

The FEA has been used to compute the magnetic field along the cross-section of the proposed generator. By the fact that, with the rare-earth magnet materials, a high magnetic field was possible to be achieved, especially, with the Halbach array configuration. However, in this study, the quasi-Halbach magnetization technique was selected for the moving-magnet, because it has the following advantages as compared with a conventional PM array [21, 22]:

- The array of PMs does not require any backing steel magnetic circuit, and the PMs can be bonded directly to a non-ferromagnetic supporting tube, such as plastics or aluminum.
- The power efficiency of the machine will be doubled because the fundamental field is stronger by a factor of 1.4 than in a conventional PM array.
- As compared to a conventional PM array, the magnetic field is more sinusoidal.

The picture of the Halbach array is shown in Fig.1 (a), and Fig.1 (b) shows the representation of the generated flux from the quasi-Halbach [21, 23].

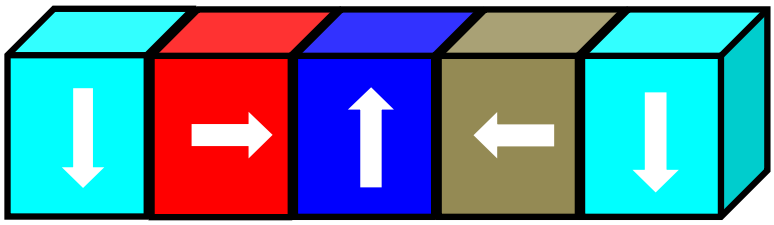

(a) Five PM-ring quasi-Halbach array

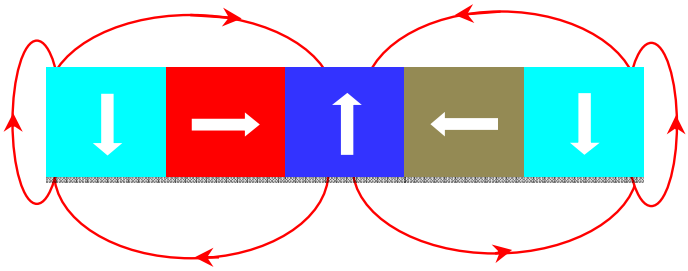

(b) Magnet flux distributions of the Halbach array magnets

Fig. 1. Quasi-Halbach magnetization and its magnetic flux distributions

The finite element two-dimensional (2-D) and three-dimensional (3-D) models adopted from ANSYS Maxwell simulation software for the proposed PMLG with laminated silicon steel and Somaloy stator core are shown in Fig. 2 and Fig. 3, respectively. The FPLG with single phase and long translator. It contains 6 coils and 6 slots. The translator is made of the neodymium-iron-boron (NdFeB) permanent magnet and it consists series of quasi-Halbach magnetized magnets. Quasi-Halbach magnetization provides higher air gap magnetic field distribution [24, 25]. The FEA is carried out for the PMLG with both materials; an axisymmetrical coordinate system with vector orientation for magnets has been adopted for the calculations.

The FE mesh affects the FEA calculation, especially in terms of time and accuracy of the computation. Thus, when the automatic mesh was used, allowed for a faster simulation and shorter execution time than a fine mesh. Nevertheless, the computation accuracy is low because the number of degrees of freedom is low [26]. Therefore, the fine mesh has been assigned for both proposed designs. It can be concluded that, the automatic mesh is suitable for fast computing, but with low accuracy; whereas, the fine mesh is suitable for high accuracy, but the computing process will be slow.

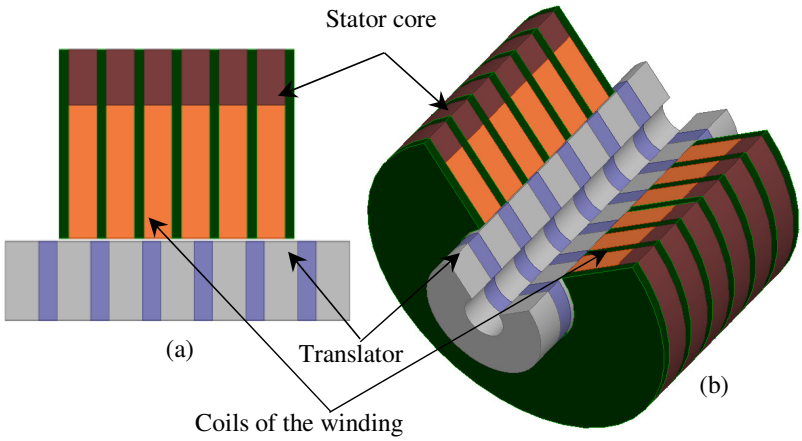

Fig. 2. Configuration of proposed PMLG with silicon steel lamination stator core (a) two-dimensional (b) three-dimensional

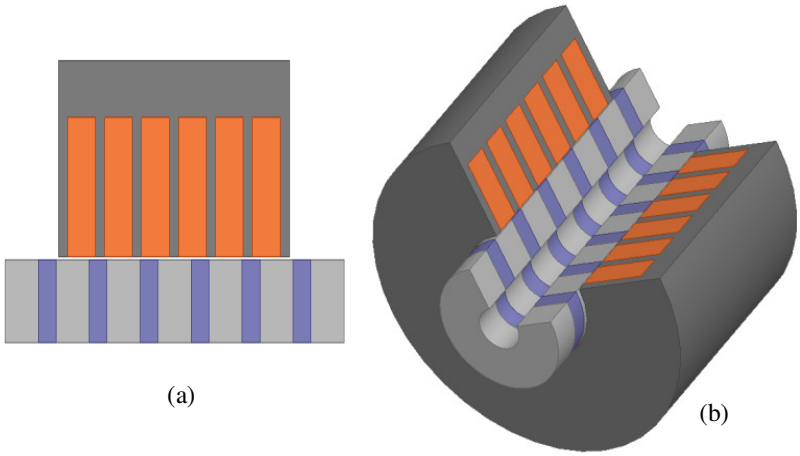

Fig. 3. Configuration of proposed PMLG with Somaloy stator core (a) two-dimensional (b) three-dimensional

Therefore, the magnetic field analysis is confined to two regions, namely the airspace region in which the permeability is μ_0, and the magnetic region in which the permeability is $\mu_0\mu_r$, μ_r being the relative recoil permeability which for rare-earth PMs is close to unity. Therefore, for the magnetic flux density, B in airspace region and magnetic region, respectively, can be expressed as [27, 28]

$$B = \mu_0 H \tag{1}$$

$$B = \mu_0 \mu_r H + \mu_0 M \tag{2}$$

The magnetization, M of the linear machine in the cylindrical coordinate system can be expressed as [27, 29, 30]

$$M = M_r e_r + M_z e_z \tag{3}$$

The magnetization distribution was expandable into Fourier series, with M_r and M_z expressed as a function of z as in (4) and (5), respectively [14, 29].

$$M_r = \sum_{n=1,2,\ldots}^{\infty} M_{rn} \cos m_n z \tag{4}$$

$$M_z = \sum_{n=1,2,\ldots}^{\infty} M_{zn} \sin m_n z \tag{5}$$

where M_r and M_z denoted the components of M in the radially and axially directions, respectively, and $m_n = 2\pi n / T_{lp}$.

When the flux waveform is known, it can be used to calculate the open-circuit voltage of the motor. Therefore, with a time-varying magnetic flux, $\phi(t)$, the induced voltage can be calculated as [23, 31]:

$$e_c = -\frac{d\phi(t)}{dt} = -\frac{dB}{dt} A \tag{6}$$

where B is the magnetic flux density and A is the area that is occupying B. On the other hand, the thrust force for a given motor current can also be calculated from the electromagnetic power as the product of the EMF and winding current divided by the translator speed, v_t. Therefore, F_T is quantified as in (7) [29, 32]:

$$F_T = \frac{e_c i_a}{v_t} = K_E(z_d) i_a = K_T(z_d) i_a \tag{7}$$

The dynamics of the system governing the armature movement of the proposed motor along the z-axis when the mass, M_m, is moving at speed; v_t with a damping coefficient, b, and spring elasticity, k, based on Alembert's equation can be expressed as [33, 34]:

$$M_m \frac{dv_t}{dt} + b v_t + k \int v_t dt = K_T(z_d) i_a \tag{8}$$

By substituting the value of F_T from (7), equation (8) can be rewritten as:

$$M_m \frac{dv_t}{dt} + bv_t + k\int v_t dt = F_T \tag{9}$$

When the linear velocity is related to the displacement and time, the velocity of the translator can be expressed as [35]:

$$v_t = \frac{dz_d}{dt} \tag{10}$$

By taking the integration of (9) and substituting the value of v_t, it results in:

$$M_m \frac{d^2 z_d}{dt^2} + b\frac{dz_d}{dt} + kz_d = F_T \tag{11}$$

where z_d, $d^2 z_d / dt^2$, K_T, i_a and dz_d / dt are the displacement of the translator, linear acceleration, thrust force constant, coil current and velocity of the translator, respectively.

The flux-linkage, ψ_c, in the winding can be obtained as

$$\psi_c = \sum_{n=1}^{\infty} \phi_c \sin m_n z_d \tag{12}$$

where

$$\phi_c = \frac{(2\pi N_c K_{rn} K_{dpn})}{m_n} \tag{13}$$

where N_c and K_{dpn} are the number of coil turns and the winding factor, respectively.

3. Results and discussion

In this study, the machine is running at no-load, the winding current is zero. The permeability into the magnets and the coils is μ_0 without demagnetization of the magnet. The magnetic properties of silicon steel lamination and Somaloy have been identified. The design specification and main dimensions of the proposed PMLG are tabulated in Table 2.

Table 2: Design specification and main dimensions of PMLG

Parameter	Value	Unit
Magnet thickness	29.50	mm
Mechanical air gap	1.00	mm
Magnetic Remanence	1.14	Tesla
Stroke	45.00	mm
The total length	221	mm

The analysis comparisons have been conducted based on two different outcomes, such as the flux line and flux density distribution in the generator. The outcomes of the analysis are further discussed as follows. Fig. 4 and Fig. 5 show the magnetostatic results for the flux lines and flux density distribution in the proposed design with silicon steel lamination using 2-D FEA. The quasi-Halbach provided the magnetization for the translator and created the flux line in round or closed loop pattern. From the indicator attached, there is a strong flux line created by the permanent magnet indicated by red and green lines. While the positive and negative value of the flux line just to illustrate the complete loop. Besides,

the flux density is also an important performance measure to ensure the performance of the PMLG. From Fig. 5, as per expected, the same location of strong flux lines will create strong flux density. It shows that flux lines are perpendicular with flux density. The FE mesh rebuilt at each position with refinement mesh nearly the air gap. The variation of the flux lines is from 0.00054 to 0.00054 weber, whereas the flux density varies from 0.0003 to 2.5266 T.

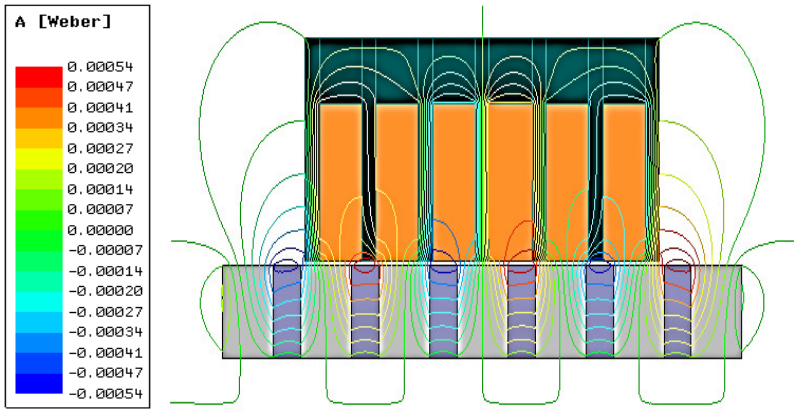

Fig. 4. Magnetic flux lines distribution with Somaloy stator core

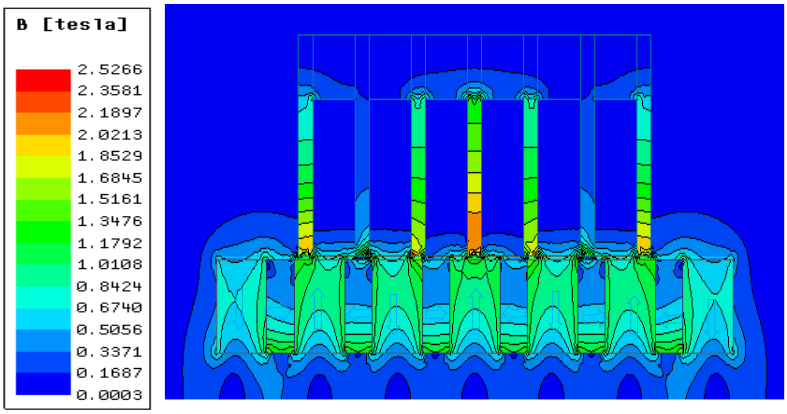

Fig. 5. Magnetic flux density distribution with Silicon steel laminations

Fig. 6 and Fig. 7 show the flux lines and flux density distributions, calculated by 2-D FEA on a generator in which the translator has quasi-Halbach magnetized magnets and stator core made of Somaloy. The flux lines vary from 0.00054 to 0.00054 weber as can be observed, there is no difference between the flux lines in the generator for both materials, because the calculation has been carried at no load and there is no effect of the core material. The variation of the flux density is from 0.0004 to 2.8247 T, it can be observed more magnetic flux density has been distributed in the generator with Somaloy core.

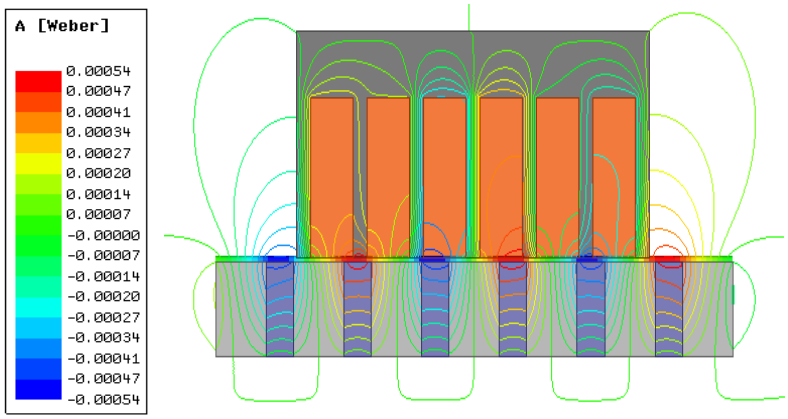

Fig. 6. Magnetic flux lines distribution with Somaloy core

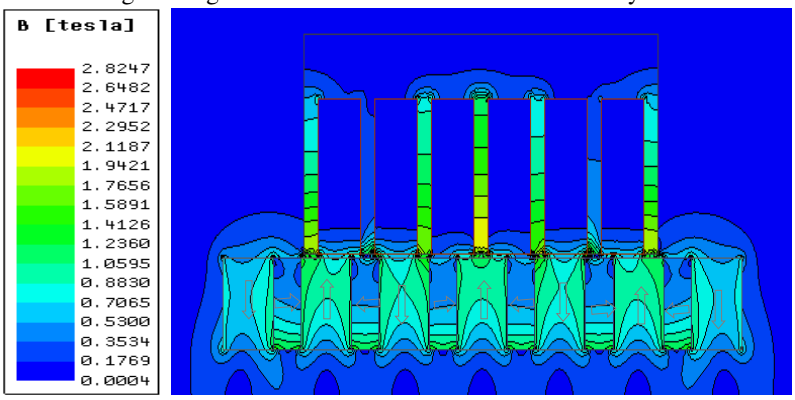

Fig. 7. Magnetic flux density distribution with Somaloy core

The comparison of the air gap magnetic flux density at zero translator's displacement is shown in Fig. 8. It will be seen that, it is not much difference between the two ferromagnetic materials are used for the stator core of the PMLG, as average magnetic flux density of 0.7733 tesla and 0.7707 tesla have been obtained for silicon steel lamination and Somaloy, respectively. The same translator has been used in both cases.

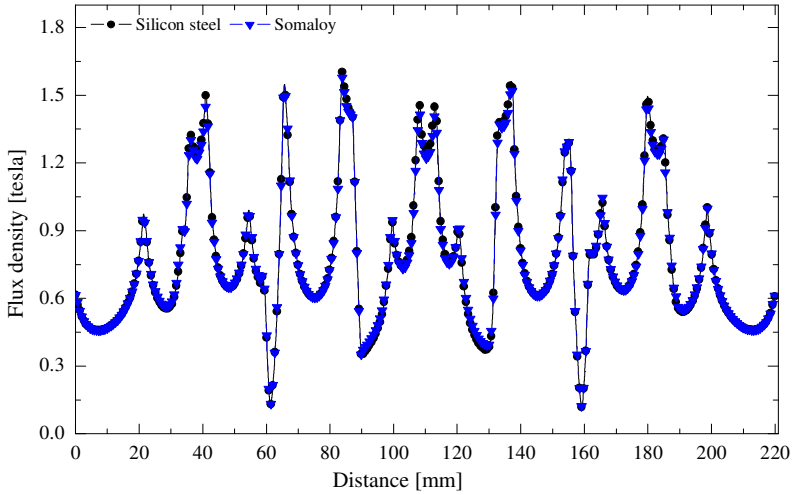

Fig. 8. Comparison of the air gap magnetic flux distribution of the proposed PMLG with silicon steel lamination and Somaloy stator cores.

The back-electromotive force (B-EMF) is a very useful parameter in the design of electrical machines because it enables the designer of estimating the efficiency and thrust

force. The amount of the magnetic flux which is developed by the magnets and links the winding is used to calculate the B-EMF of the machine. Fig. 9 shows the comparison of the B-EMF of the generator with both ferromagnetic materials. Moreover, Table III gives the comparison of rms B-EMF and average B-EMF for the generator with the materials that have been used for the stator core. It can be seen that the generator with Somaloy gives better performance.

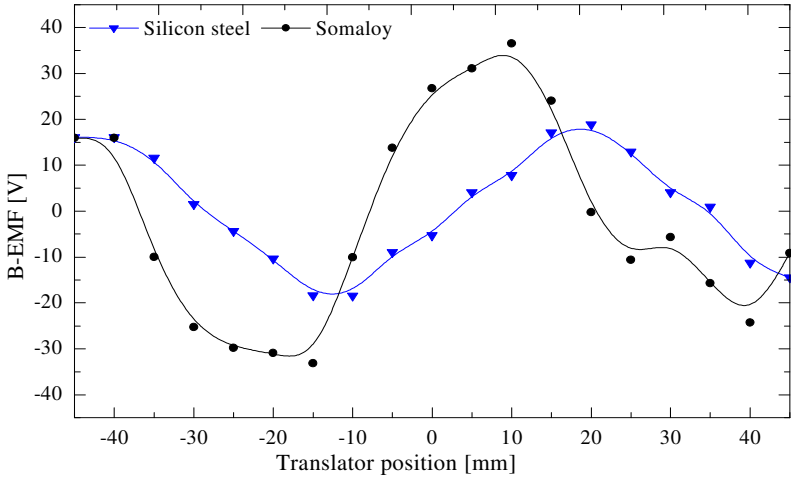

Fig. 9. Comparison of no-load B-EMF waveforms at 1 m/s

Table 3: Comparison of B-EMF of PMLG with silicon steel lamination and Somaloy stator core

Material	rms B-EMF	Average B-EMF
Silicon steel	13.32 V	10.55 V
Somaloy	25.85 V	12.23 V

Fig. 10 shows the comparison of flux-linkage in the winding of the generator for both, with silicon steel and Somaloy, it can be observed that the generator with Somaloy has a higher flux-linkage. Furthermore, Table 4 gives the average value and rms value of flux-linkage in the two cases.

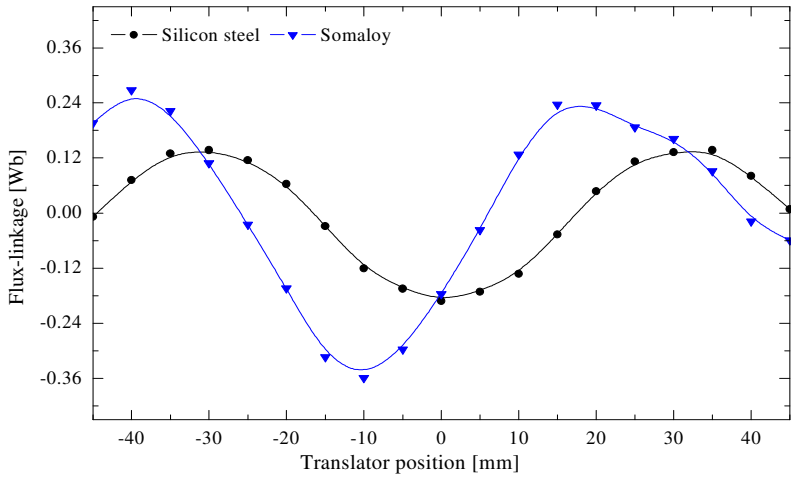

Fig. 10. Comparison of no-load flux-linkage at 1 m/s

Table 4: Comparison of flux-linkage of PMLG with silicon steel lamination and Somaloy stator core

Material	rms flux-linkage	Average flux-linkage
Silicon steel	0.1165 wb	0.0093 wb
Somaloy	0.1323 wb	0.0203 wb

Winding inductance also one of the performance measures for the electrical machine, therefore, Fig. 11 shows the comparison of the winding inductance for the proposed PMLG, it can be observed that, the PMLG with Somaloy has higher winding inductance than the generator with silicon steel lamination.

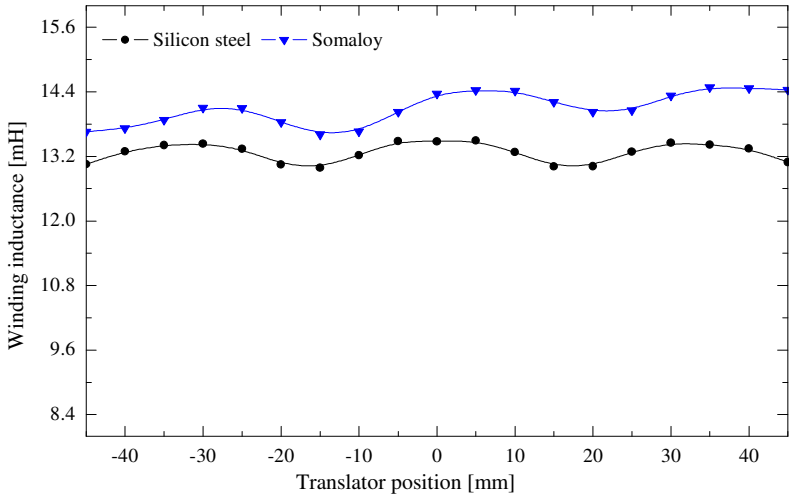

Fig. 11. Comparison of winding inductance for the generator with two different stator core materials

Cogging force in the PMLG leads to oscillations of the generator speed and therefore output voltage and power fluctuations. The cogging force corresponds to the force due to the shape of the teeth and the permanent magnets when the current in the coil of the machine is zero. This force its evaluation is very sensitive to the mesh. However, the preferred and accurate method to compute the cogging force, is the use of the transient solver with motion; because the mesh will remain unchanged for all the positions. Therefore, the stator is fixed and the translator will move with steps. Thus, only the magnetic field from the magnets is exist and then the effect of the slot will present. As the translator of the FPLG moved forward and backward, this effect was computed by using the FEA. Fig. 12 to Fig. 14 show the comparison of the cogging force resulted between the stator and moving magnet of the translator at different translator acceleration and under two different ferromagnetic materials for the stator core. The result is fluctuating between the positive and negative value of force. The result shows that the cogging force is reduced in the case of using Somaloy for a stator core of the PMLG at velocities 0.6 m/s, 1.0 m/s and 2.0 m/s, respectively.

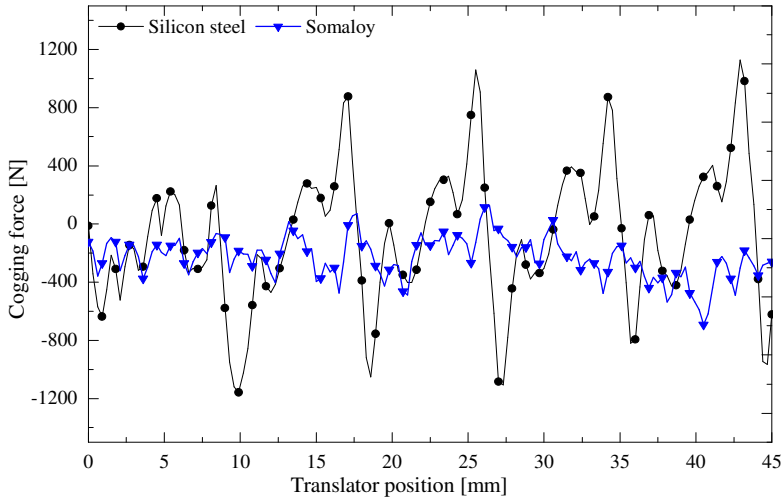

Fig. 12. Comparison of the tangential electromagnetic force component when the excitation current is zero and 45.0 mm displacement of the translator, under a linear velocity of 0.6 m/s.

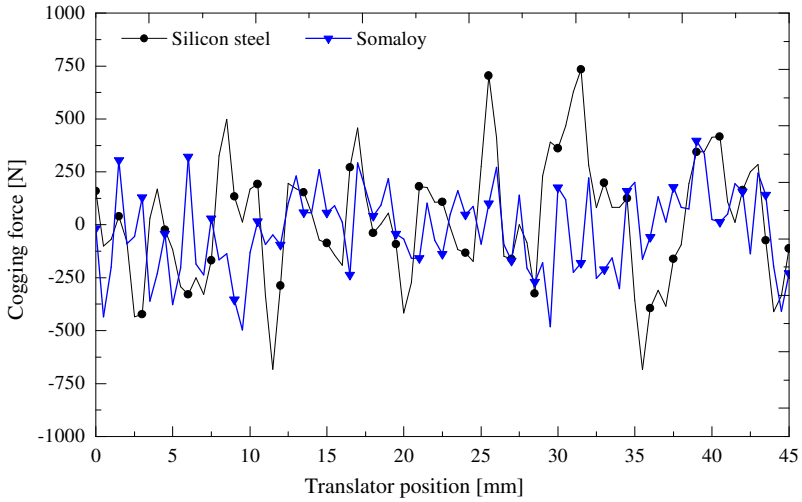

Fig. 13. Comparison of the tangential electromagnetic force component when the excitation current is zero and 45.0 mm displacement of the translator, under a linear velocity of 1 m/s.

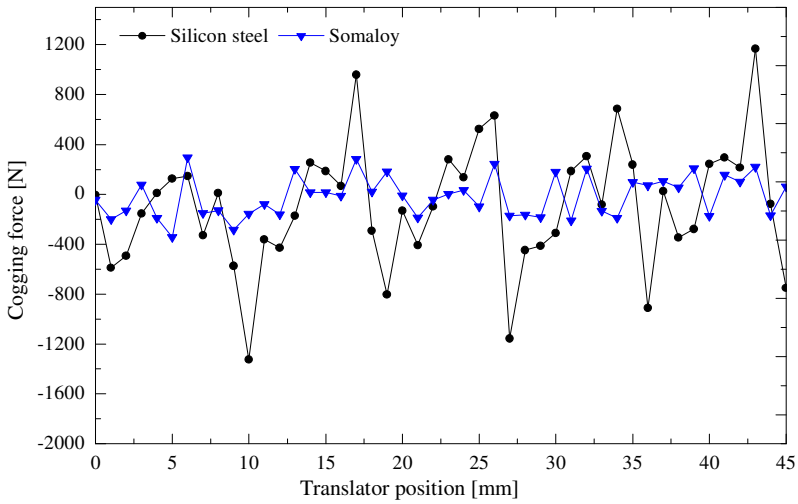

Fig. 14. Comparison of the tangential electromagnetic force component when the excitation current is zero and 45.0 mm displacement of the translator, under a linear velocity of 2 m/s.

Therefore, the cogging force reduction in the proposed design with Somaloy stator core as compared with previous published similar design [36-38], but with different techniques, it can be clearly observed that this proposed design is superior in the term of the cogging force reduction.

5. Conclusion

This paper investigated the influence of ferromagnetic material of the stator core on the amount of induced cogging force in a free-piston permanent magnet linear generator (PMLG). The PMLG with laminated silicon steel and Somaloy is analyzed using FEA. Electromagnetic characteristics such as open-circuit magnetic field distributions, B-EMF, flux-linkage, and magnetic flux density are analyzed and presented. The cogging force investigation is carried out for PMLG with both ferromagnetic materials along with main dimensions and specifications have been given. It is found that the properties of the material have a significant influence on the cogging force reduction. Also, the velocity of the translator influences the cogging force dramatically. Moreover, from the comparisons between the PMLG with silicon steel laminations and PMLG with Somaloy, it has been found that the PMLG Somaloy showed a superior performance over the PMLG with silicon steel laminations. There is a much reduction of the cogging force of generator, and the next challenge is to do as much as it can minimize the cogging force in order to have better performance. Further, with the check for the fabrication availability, it is found that is difficult to fabricate such generator with silicon steel laminations rather than using Somaloy.

Acknowledgment

Authors gratefully would like to thank Yayasan Universiti Teknologi PETRONAS (UTP) (0153AA-A92) and the Petroleum Research Fund (0153AB-A34) for funding this research work.

References

[1] M. v. D. HOEVEN, "CO_2 Emissions From Fuel Combustion IEA Statistics," *International Energy Agency: highlights. França,* 2013.

[2] O. Maloberti, R. Figueredo, C. Marchand, Y. Choua, D. Condamin, L. Kobylanski*, et al.*, "3-D–2-D dynamic magnetic modeling of an axial flux permanent magnet motor with soft magnetic composites for hybrid electric vehicles," *IEEE Transactions on Magnetics,* vol. 50, pp. 1-11, 2014.

[3] J. Wang and N. Baker, "A comparison of alternative linear machines for use with a direct drive free piston engine," 2016.

[4] A. E. Z. B. Zainal, "Effect of Injection Timing on the Operation of Hydrogen-Fuelled Free-Piston Linear Generator Engine during Starting," *International Journal of Automotive Engineering,* vol. 4, pp. 47-53, 2013.

[5] M. R. Hanipah, R. Mikalsen, and A. Roskilly, "Recent commercial free-piston engine developments for automotive applications," *Applied Thermal Engineering,* vol. 75, pp. 493-503, 2015.

[6] C. Guo, H. Feng, B. Jia, Z. Zuo, Y. Guo, and T. Roskilly, "Research on the operation characteristics of a free-piston linear generator: Numerical model and experimental results," *Energy Conversion and Management,* vol. 131, pp. 32-43, 2017.

[7] N. B. Hung and O. Lim, "A review of free-piston linear engines," *Applied Energy,* vol. 178, pp. 78-97, 2016.

[8] B. Jia, R. Mikalsen, A. Smallbone, Z. Zuo, H. Feng, and A. P. Roskilly, "Piston motion control of a free-piston engine generator: A new approach using cascade control," *Applied Energy,* vol. 179, pp. 1166-1175, 2016.
[9] E. Z. Z. Abidin, A. A. Ibrahim, A. R. A. Aziz, and S. A. Zulkifli, "Investigation of starting behaviour of a free-piston linear generator," *Journal of Applied Sciences,* vol. 12, p. 2592, 2012.
[10] A. A. Ibrahim, A. R. A. Aziz, Z. Abidin, Z. Ezrann, and S. A. Zulkifli, "Operation of Free-Piston Linear-Generator Engine Using MOSFET and IGBT Drivers," *Journal of Applied Sciences,* pp. 1-6, 2011.
[11] R. Mikalsen and A. Roskilly, "The control of a free-piston engine generator. Part 1: Fundamental analyses," *Applied Energy,* vol. 87, pp. 1273-1280, 2010.
[12] Z. A. Ezrann Z., A. I. Abdulwehab, A. A. A. Rashid, Saiful A., and Zulkifli, "Effect of Motoring Voltage on Compression Ratio of a Free-Piston Linear Generator Engine," *Journal of Mechanical Engineering and Sciences,* vol. 8, pp. 1393-1400, 2015.
[13] S. W. Youn, J. J. Lee, H. S. Yoon, and C. S. Koh, "A new cogging-free permanent-magnet linear motor," *IEEE Transactions on Magnetics,* vol. 44, pp. 1785-1790, 2008.
[14] I. I. Abdalla, T. Ibrahim, and N. B. M. Nor, "Development and optimization of a moving-magnet tubular linear permanent magnet motor for use in a reciprocating compressor of household refrigerators," *International Journal of Electrical Power & Energy Systems,* vol. 77, pp. 263-270, 2016.
[15] N. Gargov and A. Zobaa, "Multi-phase air-cored tubular permanent magnet linear generator for wave energy converters," *IET Renewable Power Generation,* vol. 6, pp. 171-176, 2012.
[16] C. Yuan, H. Feng, and Y. He, "An experimental research on the combustion and heat release characteristics of a free-piston diesel engine generator," *Fuel,* vol. 188, pp. 390-400, 2017.
[17] Y. Sui, P. Zheng, B. Yu, L. Cheng, and Z. Liu, "Research on a tubular yokeless linear PM machine," *IEEE Transactions on Magnetics,* vol. 51, pp. 1-4, 2015.
[18] J. F. Gieras, Z. J. Piech, and B. Z. Tomczuk, *Linear synchronous motors: transportation and automation systems* vol. 20: CRC press, 2012.
[19] I. I. Abdalla, T. Ibrahim, and N. M. Nor, "Linear permanent magnet motor for reciprocating compressor applications," in *2013 IEEE 7th International Power Engineering and Optimization Conference (PEOCO)*, 2013, pp. 29-34.
[20] S. Wiak, E. Napieralska-Juszczak, J. Janssen, J. Paulides, and E. Lomonova, "3D analytical field calculation using triangular magnet segments applied to a skewed linear permanent magnet actuator," *COMPEL-The international journal for computation and mathematics in electrical and electronic engineering,* vol. 29, pp. 984-993, 2010.
[21] Q. Han, "Analysis and modeling of the EDS maglev system based on the Halbach permanent magnet array," Doctor of Philosophy, Department of Electrical and Computer Engineering University of Central Florida Orlando, Florida, Orlando, Florida 2004.
[22] J. F. Gieras, R.-J. Wang, and M. J. Kamper, *Axial flux permanent magnet brushless machines* vol. 1: Springer, 2008.
[23] L. Dall'Ora, "Analysis and Design of a Linear Tubular Electric Machine for Free-piston Stirling Micro-cogeneration Systems," 2014.
[24] I. I. Abdalla, T. B. Ibrahim, and N. M. Nor, "A Study on Different Topologies of the Tubular Linear Permanent Magnet Motor Designed for Linear Reciprocating Compressor Applications," *Applied Computational Electromagnetics Society Journal,* vol. 31, 2016.
[25] I. I. Abdalla, T. Ibrahim, and N. B. M. Nor, "The Fabrication and Characterization of Short-Stroke Tubular Linear Permanent-Magnet Motor," *9th International Conference on Robotic, Vision, Signal Processing and Power Applications*, 2017, pp. 777-789.
[26] B. Silwal, "Computation of eddy currents in a solid rotor induction machine with 2-D and 3-D FEM," 2012.
[27] K. J. Meessen, B. Gysen, J. Paulides, and E. A. Lomonova, "Halbach permanent magnet shape selection for slotless tubular actuators," *IEEE Transactions on Magnetics,* vol. 44, pp. 4305-4308, 2008.
[28] N.-C. Tsai and C.-W. Chiang, "Design and analysis of magnetically-drive actuator applied for linear compressor," *Mechatronics,* vol. 20, pp. 596-603, 2010.
[29] J. Wang, D. Howe, and Z. Lin, "Comparative study of winding configurations of short-stroke, single phase tubular permanent magnet motor for refrigeration applications," *42nd Industry Applications Conference, IAS Annual Meeting. Conference Record of the 2007 IEEE*, pp. 311-318.
[30] I. I. Abdalla, T. Ibrahim, and N. M. Nor, "Design Validation of a Moving-Magnet Tubular Linear Permanent Magnet Motor with a Trapezoidal Permanent Magnet Shape," *Applied Mechanics and Materials,* vol. 793, pp. 274-279, 2015.
[31] H. Feng, Y. Song, Z. Zuo, J. Shang, Y. Wang, and A. P. Roskilly, "Stable Operation and Electricity Generating Characteristics of a Single-Cylinder Free Piston Engine Linear Generator: Simulation and Experiments," *Energies,* vol. 8, pp. 765-785, 2015.
[32] S. Vaez-Zadeh and A. H. Isfahani, "Multiobjective design optimization of air-core linear permanent-magnet synchronous motors for improved thrust and low magnet consumption," *IEEE transactions on magnetics,* vol. 42, pp. 446-452, 2006.
[33] B. Tomczuk and M. Sobol, "A field-network model of a linear oscillating motor and its dynamics characteristics," *IEEE Transactions on Magnetics,* vol. 41, pp. 2362-2367, 2005.

[34] J. Chen, Y. Liao, C. Zhang, and P. Sun, "Design of a cylindrical moving core small linear PM oscillatory actuator," *17th International Conference on Electrical Machines and Systems (ICEMS),* 2014, pp. 2211-2215.
[35] H. M. Hasanien, "Particle swarm design optimization of transverse flux linear motor for weight reduction and improvement of thrust force," *IEEE Transactions on Industrial Electronics,* vol. 58, pp. 4048-4056, 2011.
[36] J. Faiz, M. Ebrahimi-Salari, and G. Shahgholian, "Reduction of cogging force in linear permanent-magnet generators," *IEEE Transactions on Magnetics,* vol. 46, pp. 135-140, 2010.
[37] J. Si, H. Feng, P. Su, and L. Zhang, "Design and analysis of tubular permanent magnet linear wave generator," *The Scientific World Journal,* vol. 2014, 2014.
[38] D. Li, B. Bai, Q. Yu, and D. Chen, "Cogging force minimization in a permanent magnet linear generator for sea wave energy extraction applications," *International Conference on Energy and Environment Technology, ICEET'09.*, 2009, pp. 552-554.